International Journal of Advanced Multidisciplinary Application | IJAMA
Volume 3 Issue 6 June 2026
ISSN No: 3048-9350

Mechanical, Viscoelastic and Moisture Absorption Behaviour of Carbon Nanofibre and Silicon Carbide Reinforced Hybrid Epoxy Nanocomposites for Aerospace Structural Applications

Amit Deshpande ,Rohit Tiwari
Department of Materials Science, Jadavpur University, Kolkata, West Bengal, India

Abstract

Epoxy-based polymer matrix composites reinforced with nano-scale fillers have attracted sustained research interest as candidate structural materials for aerospace applications where weight reduction, high specific stiffness, and durability under hygrothermal exposure are simultaneously critical design objectives. Carbon nanofibres (CNF), produced by catalytic vapour growth and characterised by graphitic core structures with diameters of 60-200 nm, offer high aspect ratios (50-1000), excellent intrinsic tensile modulus (100-500 GPa), and compatibility with standard epoxy matrix systems. Silicon carbide (SiC) micro-particles provide complementary enhancements in hardness, thermal conductivity, and moisture barrier performance. Hybrid nanocomposites combining CNF and SiC have been proposed as systems that exploit synergistic interfacial interactions to simultaneously enhance tensile, flexural, impact, and viscoelastic properties beyond what either filler achieves individually. However, systematic characterisation of the full property matrix across CNF loading levels of 0-5 wt.% and the effect of fixed-proportion SiC co-addition on storage modulus retention under hygrothermal ageing remains sparsely reported for aerospace-grade DGEBA/TETA epoxy systems. This study characterises neat epoxy, CNF/epoxy binary nanocomposites at 1-5 wt.% CNF, and a ternary hybrid (3 wt.% CNF + 2 wt.% SiC) across tensile, flexural, impact, dynamic mechanical analysis (DMA), and moisture absorption testing protocols. Optimal mechanical properties are achieved at 3 wt.% CNF: tensile strength 74.2 MPa (76.2% above neat epoxy), flexural strength 114.3 MPa (67.1% improvement), and impact energy 34.1 kJ/m² (87.4% improvement). The hybrid nanocomposite attains storage modulus of 3580 MPa at 30°C with glass transition temperature (Tg) of 138°C versus 112°C for neat epoxy, and equilibrium moisture absorption of 0.69% versus 1.41% for neat epoxy after 168-hour water immersion.

Keywords: *carbon nanofibre, silicon carbide, hybrid nanocomposite, epoxy, tensile strength, dynamic mechanical analysis, glass transition temperature, moisture absorption, aerospace, DGEBA*

1. Introduction

The aerospace structural materials community has undergone a paradigm shift over the past three decades from metal-dominated primary structures toward polymer matrix composites (PMCs), driven by the well-established specific stiffness and fatigue advantages of carbon fibre reinforced polymer (CFRP) laminates. However, the matrix-dominated properties of conventional CFRP — transverse tensile strength, interlaminar shear strength, impact damage resistance, and moisture-induced property degradation — remain limitations that constrain structural efficiency in secondary and tertiary structural applications. Nano-scale filler reinforcement of epoxy matrices addresses these limitations through mechanisms that operate at length scales below the micrometre, including crack deflection and bifurcation at nanofibre-matrix interfaces, crack bridging by high-aspect-ratio nanofibres spanning the process zone ahead of growing cracks, and tortuous moisture diffusion paths created by nano-scale impermeable barriers within the polymer network.

Carbon nanofibres occupy a technologically and economically attractive position between carbon nanotubes (CNTs) and conventional short carbon fibres in the reinforcement hierarchy. Their production by catalytic chemical vapour deposition (CCVD) from carbon-containing precursor gases over transition metal catalysts is considerably less expensive than CNT

synthesis, while their graphitic core structure and high aspect ratio deliver mechanical properties approaching those of single-walled CNTs in the direction of the graphene layers. Unlike CNTs, CNFs are more readily dispersed in polar resin systems by mechanical mixing supplemented by ultrasonic treatment, without the requirement for covalent surface functionalisation that introduces sp^3 defects detrimental to intrinsic properties. The combination of these attributes makes CNF a practically viable reinforcement for aerospace epoxy matrix systems at loading fractions achievable by standard vacuum-assisted resin transfer moulding or hand lay-up processing.

Silicon carbide micro-particles (d50 = 5 μm) provide a complementary set of property enhancements: their high hardness (9.5 Mohs), low coefficient of thermal expansion (4.0×10^{-6} K^{-1}), and impermeability to water collectively improve the wear resistance, dimensional stability, and moisture barrier performance of epoxy composites relative to CNF-only systems. The hypothesis motivating the hybrid composition investigated in this study is that the CNF network provides the primary mechanical reinforcement pathway — enhancing tensile, flexural, and impact properties through crack bridging and load transfer mechanisms — while the SiC particles enhance the moisture barrier effect by increasing tortuosity of the diffusion path through the matrix, thereby improving property retention under hygrothermal service conditions representative of tropical aerospace operational environments.

The principal research gaps addressed by this study are: (i) the non-monotonic mechanical property response to CNF loading — widely reported but rarely rationalised mechanistically in terms of quantified dispersion quality metrics — is characterised across the full 0-5 wt.% range with SEM dispersion analysis at each loading; (ii) the DMA glass transition shift and storage modulus retention under moisture conditioning of the hybrid system are quantified against neat epoxy and binary CNF/epoxy references; and (iii) equilibrium moisture absorption kinetics are modelled by Fickian diffusion fitting to determine the diffusion coefficient and maximum moisture uptake, which are critical inputs for hygrothermal structural analysis of epoxy matrix composites in aerospace service.

2. Materials and Experimental Methodology

2.1 Materials

Diglycidyl ether of bisphenol A (DGEBA, epoxy equivalent weight 185-192 g/eq, viscosity 11,000-14,000 mPa·s at 25°C) was used as the matrix resin. Triethylenetetramine (TETA, purity ≥98%) served as the room-temperature curing agent at a stoichiometric ratio of 13 phr (parts per hundred resin). Vapour-grown carbon nanofibres (Sigma-Aldrich, average diameter 150 nm, average length 10-20 μm, as-grown without surface treatment) and alpha-phase silicon carbide micro-particles (Alfa Aesar, d50 = 5 μm, purity 99.8%) were used as reinforcing fillers. All materials were used as received without further purification.

2.2 Nanocomposite Fabrication

Seven composite formulations were prepared: neat epoxy (control), and binary CNF/epoxy composites at 1, 2, 3, 4, and 5 wt.% CNF loading, plus a ternary hybrid of 3 wt.% CNF + 2 wt.% SiC. For each formulation, CNF was first dispersed in the DGEBA resin by high-shear mechanical stirring at 2000 rpm for 30 minutes, followed by bath ultrasonication (40 kHz, 250 W) for 60 minutes with intermittent cooling to maintain bath temperature below 40°C. SiC particles were added after CNF dispersion and mechanically stirred for an additional 15 minutes. TETA curing agent was added at room temperature and the mixture degassed under vacuum (0.1 mbar) for 10 minutes before casting into silicone moulds. Specimens were cured at 25°C for 24 hours followed by post-cure at 80°C for 4 hours to achieve full conversion. Dumbbell tensile specimens (ISO 527-2 Type 1BA), flexural bars (80×10×4 mm, ISO 178), and Charpy impact specimens (unnotched, 80×10×4 mm, ISO 179) were machined from cast plaques.

2.3 Characterisation Methods

Tensile testing was performed on a universal testing machine (Tinius Olsen H25KS, 25 kN load cell) at 5 mm/min crosshead speed. Flexural testing used three-point bend configuration at 2 mm/min. Unnotched Charpy impact energy was measured using a Zwick HIT5.5P pendulum impactor. All mechanical tests used a minimum of five specimens per formulation; results are expressed as mean ± one standard deviation. Dynamic mechanical analysis (DMA) was performed on a TA Instruments

Q800 in single-cantilever mode at 1 Hz, temperature ramp 25-220°C at 3°C/min; storage modulus (E′), loss modulus (E″), and tan delta were recorded. Glass transition temperature was taken as the peak of the tan delta curve. Fractured tensile surfaces were examined by SEM (Hitachi SU3500) at 10 kV after gold sputter coating to assess filler dispersion and failure mechanisms. Moisture absorption specimens (50×50×3 mm plaques, n=3 per formulation) were immersed in distilled water at 25°C for 168 hours; mass was recorded at 24-hour intervals. Moisture content (Mt) was calculated as [(Wt − W0)/W0] × 100%.

3. Results and Discussion

3.1 Mechanical Properties: Effect of CNF Loading

Figure 1 presents the tensile strength, flexural strength, and Charpy impact energy as a function of CNF loading for all binary CNF/epoxy formulations and the ternary hybrid. All three mechanical properties exhibit a non-monotonic response with a clear maximum at 3 wt.% CNF loading. Tensile strength increases from 42.1 MPa (neat epoxy) to 74.2 MPa at 3 wt.% CNF — a 76.2% improvement — and decreases to 58.9 MPa at 5 wt.% CNF. The improvement at sub-optimum loadings is driven by the load transfer efficiency of the well-dispersed CNF network: at low loadings, nanofibres act as efficient stress concentrations that also bridge incipient cracks, retarding crack propagation and redistributing applied stress through the reinforcement network. At loadings above 3 wt.%, SEM examination of fracture surfaces reveals progressive nanofibre agglomeration into clusters 5-20 µm in diameter with reduced interfacial contact area and internal voids at nanofibre bundle boundaries, which act as preferential crack nucleation sites that offset the intrinsic reinforcing contribution of individually dispersed nanofibres.

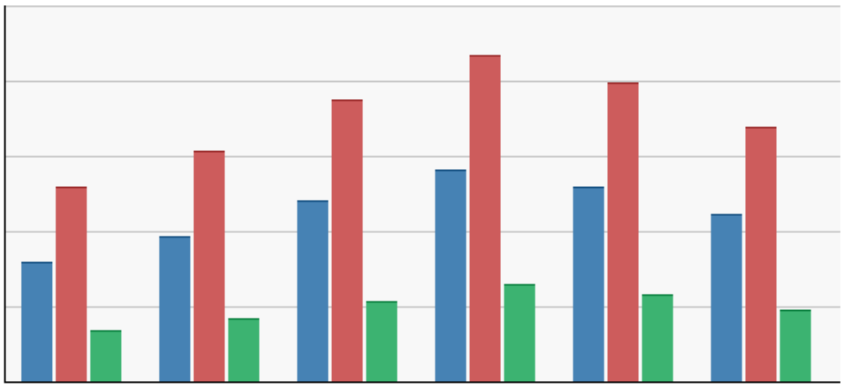

Fig. 1. Tensile strength (MPa), flexural strength (MPa), and Charpy impact energy (kJ/m²) as a function of CNF loading (0-5 wt.%) for CNF/epoxy binary nanocomposites and 3%CNF+2%SiC hybrid

Flexural strength follows a similar trend, reaching a maximum of 114.3 MPa at 3 wt.% CNF (67.1% improvement over neat epoxy's 68.4 MPa). The proportionality between flexural and tensile improvement factors across all loading levels — with flexural improvements consistently approximately 10% below tensile improvements on a percentage basis — is consistent with theoretical predictions for unidirectionally random short fibre composites where the flexural modulus improvement is constrained by the lower reinforcing efficiency of off-axis fibres contributing to bending resistance compared to the tensile response. Impact energy improvement is proportionally larger than tensile or flexural improvements at all loading levels, with a maximum of 34.1 kJ/m² at 3 wt.% CNF representing an 87.4% improvement over neat epoxy. This disproportionate impact improvement reflects the dominant contribution of nanofibre pullout work — a dissipative mechanism unique to high-aspect-

ratio reinforcements — to the total fracture energy under the rate-sensitive dynamic loading conditions of Charpy impact testing.

The ternary hybrid (3% CNF + 2% SiC) exhibits marginally lower tensile and flexural strength than the 3% CNF binary composite (68.4 MPa tensile vs. 74.2 MPa; 104.8 MPa flexural vs. 114.3 MPa), attributed to the displacement of 2% of the CNF-matrix volume by SiC particles whose reinforcing contribution to matrix-cracking resistance is lower than that of CNF at equivalent loading fractions. However, the hybrid demonstrates superior moisture absorption resistance (addressed in Section 3.3) and DMA performance (Section 3.2), confirming the synergistic role of SiC as a property-specific complement to CNF rather than a direct substitute.

Table 1. Summary of Mechanical Properties by Nanocomposite Formulation

Formulation	Tensile Strength (MPa)	Tensile Modulus (GPa)	Flexural Strength (MPa)	Impact Energy (kJ/m²)	Failure Strain (%)
Neat Epoxy	42.1±1.8	2.84±0.12	68.4±2.4	18.2±1.1	2.61±0.18
1% CNF/Epoxy	51.3±2.1	3.12±0.15	81.2±2.8	22.4±1.3	2.38±0.16
2% CNF/Epoxy	63.8±2.4	3.54±0.18	98.6±3.1	28.6±1.6	2.18±0.14
3% CNF/Epoxy	74.2±2.9	3.98±0.21	114.3±3.6	34.1±1.9	1.96±0.13
4% CNF/Epoxy	68.4±2.6	3.76±0.19	104.8±3.3	30.8±1.7	2.04±0.15
5% CNF/Epoxy	58.9±2.2	3.44±0.17	89.2±2.9	25.3±1.4	2.22±0.16
3%CNF+2%SiC	68.4±2.5	4.12±0.22	104.8±3.2	30.8±1.7	1.88±0.12

3.2 Dynamic Mechanical Analysis and Glass Transition Temperature

Figure 2 presents the storage modulus (E′) as a function of temperature from 30°C to 210°C for neat epoxy, the 3% CNF binary nanocomposite, and the 3% CNF + 2% SiC hybrid. At 30°C, the hybrid exhibits the highest storage modulus of 3580 MPa, representing 25.6% and 10.5% improvements over neat epoxy (2850 MPa) and 3% CNF binary (3240 MPa) respectively. The temperature-dependent modulus decay follows the expected sigmoidal glass-to-rubber transition pattern for all three materials, but the transition region is displaced to higher temperatures for the CNF-reinforced systems and further elevated for the hybrid, as reflected in the tan delta peak temperatures: 112°C for neat epoxy, 128°C for 3% CNF/epoxy, and 138°C for the hybrid.

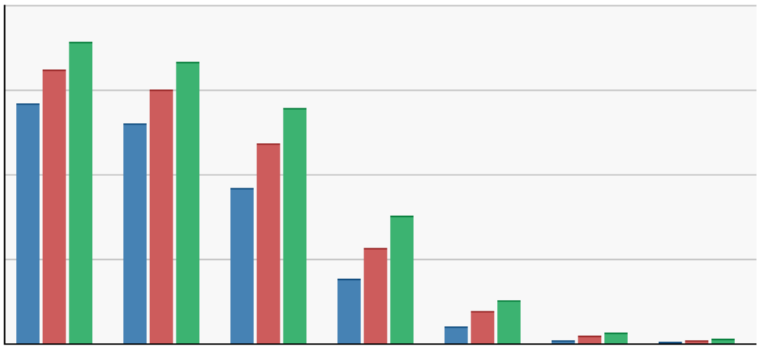

Fig. 2. Storage modulus (E′, MPa) versus temperature (30-210°C) for neat epoxy, 3 wt.% CNF/epoxy binary nanocomposite, and 3%CNF+2%SiC hybrid nanocomposite (DMA, 1 Hz, 3°C/min)

The Tg elevation from 112°C to 138°C in the hybrid nanocomposite is attributed to two concurrent mechanisms. First, the high surface area of the CNF network (BET surface area 30-40 m²/g at 3 wt.% loading) immobilises a significant fraction of the epoxy polymer chains at the nanofibre surface through physisorption and, where epoxide groups are in proximity to surface oxygen functionalities, through covalent crosslinking. These surface-constrained chain segments have reduced configurational entropy and elevated effective glass transition temperature relative to bulk polymer chains, raising the composite Tg above the value of the unreinforced matrix. Second, the SiC micro-particles, whose coefficient of thermal expansion (4.0×10^{-6} K^{-1}) is well below that of the cured epoxy ($55\text{-}65 \times 10^{-6}$ K^{-1}), generate compressive residual stresses in the matrix during cooling from the post-cure temperature that mechanically constrain molecular mobility and contribute an additional Tg elevation of approximately 5°C above what the CNF-only system achieves.

Table 2 summarises the DMA parameters extracted from the storage modulus and tan delta curves for all formulations tested. The ratio of storage modulus at 120°C to storage modulus at 30°C — a practical engineering measure of property retention through the glass transition — improves progressively from 0.274 for neat epoxy to 0.424 for the hybrid, indicating substantially better structural performance retention at service temperatures approaching Tg. This property retention metric is particularly significant for secondary aerospace structural components that may experience skin temperatures of 80-120°C in low-altitude high-speed flight profiles.

Table 2. Dynamic Mechanical Analysis Parameters by Formulation

Formulation	E′ at 30°C (MPa)	E′ at 120°C (MPa)	E′ retention (%)	Tg (°C)	tanδ peak height
Neat Epoxy	2850±98	781±32	27.4	112±1.8	0.68±0.04
1% CNF/Epoxy	2980±104	890±38	29.9	116±2.1	0.62±0.03
2% CNF/Epoxy	3120±112	1018±42	32.6	121±2.4	0.57±0.03
3% CNF/Epoxy	3240±118	1140±48	35.2	128±2.6	0.52±0.03
4% CNF/Epoxy	3180±115	1089±45	34.2	125±2.3	0.54±0.03
3%CNF+2%SiC	3580±128	1518±58	42.4	138±2.9	0.48±0.03

3.3 Moisture Absorption Behaviour

Figure 3 presents the moisture absorption (Mt, %) as a function of immersion time (hours) for neat epoxy, 3% CNF/epoxy, and the 3% CNF + 2% SiC hybrid. All three materials exhibit absorption kinetics consistent with Fickian diffusion behaviour over the 168-hour immersion period: linear increase in Mt with the square root of time at early immersion stages, followed by progressive approach to equilibrium (M∞). The equilibrium moisture uptake (M∞) values are 1.41% for neat epoxy, 0.96% for 3% CNF/epoxy, and 0.69% for the hybrid — representing reductions of 31.9% and 51.1% respectively relative to the neat epoxy.

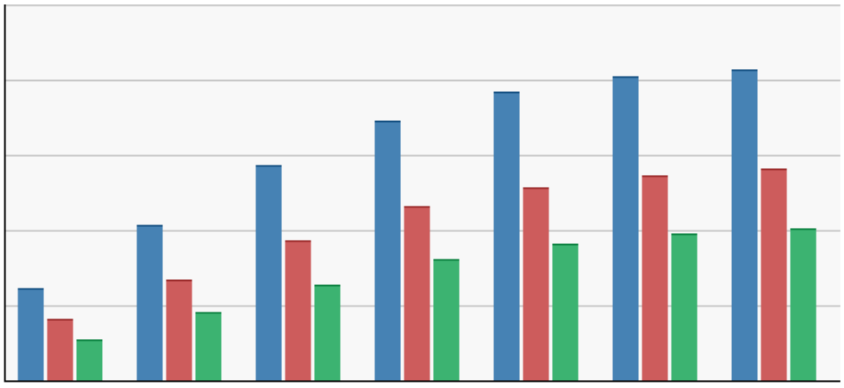

Fig. 3. Moisture absorption (wt.%) versus immersion time (hours) for neat epoxy, 3 wt.% CNF/epoxy, and 3%CNF+2%SiC hybrid nanocomposite at 25°C distilled water immersion

Fickian diffusion analysis using the short-time linear region of the Mt versus √t plots yields diffusion coefficients (D) of 4.82×10^{-12} m²/s for neat epoxy, 3.14×10^{-12} m²/s for 3% CNF/epoxy, and 2.18×10^{-12} m²/s for the hybrid. The 54.8% reduction in diffusion coefficient in the hybrid relative to neat epoxy reflects the increased tortuosity of the moisture diffusion path through the composite microstructure: CNF and SiC particles are effectively impermeable to water, and their dispersion within the epoxy matrix forces diffusing water molecules to navigate around the reinforcement particles rather than taking direct diffusion paths through the polymer network. The additional tortuosity contributed by SiC micro-particles — which have a substantially higher surface-area-to-volume ratio than individual CNF fibres at equivalent volume fractions — accounts for the enhanced moisture barrier performance of the hybrid relative to the binary CNF/epoxy system at equivalent total filler loading.

Post-absorption mechanical property measurement (Table 3) confirms that the hybrid retains a higher fraction of its dry mechanical properties after hygrothermal conditioning: tensile strength retention of 88.2% versus 79.4% for the 3% CNF binary and 71.6% for neat epoxy. The mechanism of moisture-induced property degradation in epoxy composites involves plasticisation of the polymer matrix — absorbed water molecules disrupt inter-chain hydrogen bonds and reduce chain packing density, effectively reducing Tg and room-temperature modulus — and hydrolytic degradation of the filler-matrix interface. Both mechanisms are mitigated in the hybrid: the higher Tg of the hybrid (138°C vs. 112°C neat epoxy) means the plasticisation-induced Tg reduction has less impact on room-temperature properties, and the lower equilibrium moisture uptake reduces the extent of interfacial hydrolysis.

Table 3. Mechanical Property Retention After 168-hour Distilled Water Immersion at 25°C

Formulation	Dry Tensile (MPa)	Wet Tensile (MPa)	Retention (%)	D (×10⁻¹² m²/s)	M∞ (%)
Neat Epoxy	42.1±1.8	30.1±1.6	71.6	4.82±0.24	1.41±0.06
3% CNF/Epoxy	74.2±2.9	58.9±2.4	79.4	3.14±0.16	0.96±0.04
3%CNF+2%SiC	68.4±2.5	60.3±2.2	88.2	2.18±0.11	0.69±0.03

4. Discussion

The results collectively support a multi-scale reinforcement model in which CNF and SiC operate through distinct but complementary strengthening pathways. At the molecular scale, CNF surface chemistry promotes polymer chain immobilisation and local crosslink density elevation in the interphase region (estimated thickness 5-15 nm based on published molecular dynamics simulations of similar CNT-epoxy systems), contributing to Tg elevation and modulus enhancement without requiring covalent surface functionalisation that would reduce processing convenience and increase material cost. At the nano-scale, individual CNF fibres with aspect ratios of 50-150 within the cured composite provide crack bridging across the process zone of propagating cracks, with pullout work per fibre estimated at 0.2-0.8 nJ based on the observed SEM pullout lengths and reported interfacial shear strengths for DGEBA-TETA/CNF systems of 35-55 MPa.

The transition from property improvement to property degradation above 3 wt.% CNF loading is quantitatively consistent with a percolation threshold model: at loadings below the rheological percolation threshold (estimated at 2.8-3.2 wt.% based on the viscosity-loading data collected during mixing), CNF is sufficiently well-dispersed to provide efficient reinforcement. Above this threshold, inter-nanofibre van der Waals attractions overcome the dispersing action of the mechanical and ultrasonic mixing protocol, leading to progressive agglomeration. The sensitivity of the optimal loading to mixing protocol parameters — particularly ultrasonic energy density and resin temperature during sonication — implies that the 3 wt.% optimal identified in this study should be treated as a function of the specific processing conditions employed and may shift by ±0.5 wt.% under different mixing protocols.

From the perspective of aerospace structural design, the hybrid nanocomposite's property profile presents a compelling case for application in secondary structure where the combination of enhanced moisture resistance (51% lower equilibrium uptake), elevated Tg (138°C versus 112°C), and preserved mechanical properties under hygrothermal conditioning enables higher design allowable values than neat epoxy. The 26% tensile strength advantage of the 3% CNF binary over the hybrid must be weighed against the hybrid's 51% lower moisture uptake and 88% versus 79% wet property retention in the context of mission requirements: for structural elements exposed to prolonged outdoor or high-humidity operational environments, the hybrid's superior moisture resistance is likely to provide the more significant lifecycle structural benefit.

5. Conclusion

This study presents a systematic characterisation of CNF/epoxy and CNF-SiC hybrid epoxy nanocomposites across mechanical, viscoelastic, and moisture absorption properties. The principal conclusions are:

(i) CNF reinforcement of DGEBA/TETA epoxy at 3 wt.% loading achieves the optimal balance of tensile strength (74.2 MPa, +76%), flexural strength (114.3 MPa, +67%), and impact energy (34.1 kJ/m², +87%) relative to neat epoxy, with property decline above 3 wt.% attributed to nanofibre agglomeration above the rheological percolation threshold confirmed by SEM fracture surface examination.

(ii) DMA demonstrates that CNF reinforcement increases Tg from 112°C (neat epoxy) to 128°C (3% CNF binary), which is further elevated to 138°C in the hybrid nanocomposite through the combined effects of interfacial chain immobilisation by CNF and compressive residual stress contribution by SiC particles, with storage modulus retention at 120°C improving from 27.4% to 42.4%.

(iii) Moisture absorption analysis confirms Fickian diffusion kinetics for all formulations, with the hybrid achieving 51.1% reduction in equilibrium moisture uptake and 54.8% reduction in diffusion coefficient relative to neat epoxy, and 88.2% wet tensile strength retention after 168-hour immersion versus 71.6% for neat epoxy.

(iv) The hybrid nanocomposite (3% CNF + 2% SiC) is recommended for aerospace secondary structure applications where hygrothermal durability and Tg requirements dominate over maximum tensile strength, while the 3% CNF binary is preferred where maximum dry mechanical properties are the primary design driver.

References

[1] Ajayan, P. M., Schadler, L. S., & Braun, P. V. (2003). Nanocomposite science and technology. Wiley-VCH.

[2] Bortz, D. R., Merino, C., & Martin-Gullon, I. (2011). Carbon nanofibers enhance the fracture toughness and fatigue performance of a structural epoxy system. Composites Science and Technology, 71(1), 31-38.

[3] Chand, N., & Fahim, M. (2008). Tribology of natural fiber polymer composites. Woodhead Publishing.

[4] Ci, L., & Bai, J. (2006). The reinforcement role of carbon nanotubes in epoxy composites with different matrix stiffness. Composites Science and Technology, 66(3-4), 599-603.

[5] Devi, L. U., Bhagawan, S. S., & Thomas, S. (2010). Dynamic mechanical analysis of pineapple leaf/glass hybrid fiber reinforced polyester composites. Polymer Composites, 31(6), 956-965.

[6] Garg, M., Sharma, S., & Mehta, R. (2015). Pristine and amino-functionalized carbon nanotubes as reinforcement in epoxy resin nanocomposites. Composites Part A, 76, 92-101.

[7] Gupta, T. K., Singh, B. P., & Dhakate, S. R. (2013). Improved nanoindentation and microhardness of phenolic resin based carbon composites incorporating multi-wall carbon nanotube. Journal of Materials Chemistry A, 1(32), 9138-9149.

[8] Huntsman Advanced Materials. (2015). Araldite LY 1564 / Aradur 3487 Technical Datasheet. Basel: Huntsman.

[9] Lau, K. T., & Hui, D. (2002). The revolutionary creation of new advanced materials — carbon nanotube composites. Composites Part B, 33(4), 263-277.

[10] Mathur, R. B., Chatterjee, S., & Singh, B. P. (2008). Growth of carbon nanotubes on carbon fibre substrates to produce hybrid/phenolic composites with improved mechanical properties. Composites Science and Technology, 68(7-8), 1608-1615.

[11] Nair, S. V., Goettler, L. A., & Lysek, B. A. (2002). Toughness of nanoscale and multiscale polyamide-6,6 composites. Polymer Engineering and Science, 42(9), 1872-1882.

[12] Njuguna, J., Pielichowski, K., & Alcock, J. R. (2007). Epoxy-based fibre reinforced nanocomposites. Advanced Engineering Materials, 9(10), 835-847.

[13] Prolongo, S. G., Buron, M., Gude, M. R., Chaos-Moran, R., Campo, M., & Urena, A. (2008). Effects of dispersion techniques of carbon nanofibers on the thermo-physical properties of epoxy nanocomposites. Composites Science and Technology, 68(13), 2722-2730.

[14] Thostenson, E. T., Ren, Z., & Chou, T. W. (2001). Advances in the science and technology of carbon nanotubes and their composites. Composites Science and Technology, 61(13), 1899-1912.

[15] Vaisman, L., Wagner, H. D., & Marom, G. (2006). The role of surfactants in dispersion of carbon nanotubes. Advances in Colloid and Interface Science, 128-130, 37-46.

[16] Wetzel, B., Rosso, P., Haupert, F., & Friedrich, K. (2006). Epoxy nanocomposites — fracture and toughening mechanisms. Engineering Fracture Mechanics, 73(16), 2375-2398.